Permanent deformation caused by trucks with unconventional axle configurations: An analysis based on the dissipated energy approach

Erdrick Pérez-González, *PhD student, Université Laval*

Jean-Pascal Bilodeau, *Research professional, Université Laval*

Guy Doré, *Professor, Université Laval*

Paper prepared for presentation

at the Testing and Modelling of Road and Embankment Materials Session

of the 2019 TAC-ITS Canada Joint Conference, Halifax, NS

Acknowledgements

The authors wish to acknowledge to the partners of Phase 2 of the NSERC industrial research chair on the interaction of heavy loads, climate and pavements of Université Laval (Chair i3C) for the support given to this research.

Abstract

Trucks with non-conventional axle configurations are required to transport special loads. Criteria for the analysis of the effect of this type of vehicle in pavement structures are framed in the same principles of traditional vehicles. However, conditions that must be considered, such as higher loads levels, greater numbers of wheels, possible overlapping of stresses, and lower speed of circulation, cause the use of equivalence factors to be a common practice. The dissipated energy approach is based on the calculation of a fundamental property of the structure, creating a variable independent of the load mode. This paper presents the principles for pavement analysis of the effect of non-conventional trucks based on dissipated energy. A vehicle with non-conventional axle configurations on a flexible pavement typical of the province of Quebec is studied. Critical points defined by the loading condition are described. An analytical model to predict the rate of deformation based on the accumulation of dissipated energy is introduced. Both analyses are a fundamental part of a framework based on dissipated energy to rationally study of pavements under unconventional loading conditions.

Keywords: pavements, heavy load, dissipated energy, analysis.

1. Introduction

Transport of large shipments exceeding limitations of gross vehicle weight defined by current regulations, known as super-heavy loads (SHL), can benefit the economy and the environment by reducing the costs of road freight transport and allowing the transport of non-divisible cargo. However, the main concern with the SHL is that there are potential adverse effects on the performance and condition of road infrastructure. The effect of the special axle configuration, in addition to the higher magnitude of loads, causes that the stress conditions in the pavement structure to be different from the conditions associated with hypotheses normally considered during regular pavement design and analysis. This may cause that the models currently used tend to be conservative due to the extrapolation associated with their use in these special conditions.

In the available literature, the permanent deformation of the subgrade is shown as one of the most worrying failures occurring during the passage of a super-heavy vehicle with special axle configuration (Chen et al., 2013). The objective of this paper is to present the expected behaviour of the structure, based on dissipated energy, during the passage of an SHL with a special axial configuration. The influence of the dissipated energy in the development of permanent deformation will also be discussed. An analysis based on numerical simulation will be performed, and an analytical model to predict the permanent deformation in the subgrade of pavement structures is going to be introduced.

2. Background

2.1. Loading conditions for multi-axle vehicles

Pavement analysis is normally referred to a standard axle with dual wheels and 80 kN of load, however, is well known that pavement mechanical responses are sensitive to wheel locations and the interaction between the various wheels on a given axle (ARA Inc, 2004). Given this, the most accurate representation of the load will be obtained when all loads are included as they are expected in the field. However, the inclusion of all wheels and axles of vehicles with unconventional axles in a response model would be a time-consuming endeavour. Different efforts have been made in order to simplify this representation of loads to a dimension that is applicable in a practical way.

One of the elements that most concern in the analysis is the overlapping stresses, given that this condition can have an important influence on the material response and long-term behaviour. The extension of this overlapping is significantly affected by the load configuration, load magnitude, pavement layer properties and thicknesses (Hajj et al., 2018).

The effect of the different axle configurations on the pavement mechanical response has been studied previously (Chen et al., 1996, 2013; Jooste and Fernando, 1995). The studies were focused on modelling a single load, a single-line load and multiple lines of loads (group) in the pavement with linear-elastic materials. A general conclusion of this analysis is that the influence of the axle configuration in the mechanical response under SHL and different axle configurations is considerable. The simplifications in the modelling of the loading condition can be used in the analysis; however, these simplifications will have an associated error that must be mitigated with engineering criteria.

Chen et al. (Chen et al., 1996) concluded that, for pavements loaded by a group of eight wheels, the surface displacements can increase by more than 300 percent and the compression stress in the subgrade can be almost the double when compared with the response to a double tire assembly. Therefore, the tire group generated a greater influence on the surface displacement and the vertical compression of the subgrade. On the other hand, Hajj et al. (Hajj et al., 2018) establish that stresses and strains attenuate rapidly at increasing offset from the load centre, indicating that a representative group of tires can be defined (known as “nucleus”) and use in the modelling without expecting considerable bias in the results. The “nucleus” suggests that the maximum stress level is present at the edges of this representative cluster of the load pattern. However, the higher stresses are also occurring at the first and the last axle of the nucleus(Hajj et al., 2018), given this, it can be inferred that this is a condition susceptible to the axle configuration.

The studies described above have focused on trying to simulate representative elements of the loading process defined by an SHL vehicle with unconventional configurations (i.e. principal stresses). However, the use of a more general support variable, such as dissipated energy, may give a new scope of the solution for this problem. Given that this variable can be "normalized" to a certain conceptual level, the definition of a simplified load condition that generates a dissipated energy accumulation analogous to those described when considering all loads on the model will be a simpler task. It is also expected that this option to model the loading condition implicitly mitigate the errors obtained when using simplified load models, like the ones currently available in the literature.

2.2. Dissipated Energy Principles

Under vehicular traffic, pavement materials work under cyclic loading and unloading conditions. During this process, a series of loops are generated in a stress-strain plane of reference, as shown in Figure 1. The area defined inside the hysteresis loop in the stress-strain curve describes the energy dissipated during the loading-unloading stage, this energy is released in the form of mechanical work or damage (Maggiore et al., 2014; Shen et al., 2006).

Damage, in terms of pavement engineering, can be associated with the development of fatigue cracking or permanent deformation in the materials. Each loading cycle increases the accumulation of dissipated energy and causes damage until a failure condition is reached. The dissipated energy in each loading cycle can be calculated using the following equation:

[1]

$$W_N = \int_{t_n}^{t_{n+1}} \sigma(t) \cdot \varepsilon(t) dt$$

Where W_N is the dissipated energy in cycle N; t_n is the start time of cycle N; t_{n+1} is the ending time of cycle N; $\sigma(t)$ is the stress at time t in cycle N; and $\varepsilon(t)$ is the strain at time t in cycle N.

Previous studies found that the dissipated energy is not significantly affected by the loading modes, frequency, temperature, and occurrence of rest periods (Maggiore et al., 2014; Shen et al., 2006; Van Dijk and Visser, 1977). In addition, this parameter has been used previously to study the developed of fatigue in asphalt concrete, demonstrating that its application in the analysis of pavement materials is feasible. The use of dissipated energy as a rational variable would allow describing the loading and unloading process under complex stress conditions in a way that could lead to a better definition for loads simulation, as in the development of performance models for special load cases, such as SHL with special axles configurations.

3. Methodology

Dissipated energy in the analysis of non-conventional axle configurations will be studied using in two individual phases: (1) a computational simulation, aimed at quantifying the mechanical response of a pavement structure under SHL; and (2) a coupling between laboratory measurements and a full-scale test, using a heavy vehicle simulation (HVS). Aiming in this second phase, the development of a permanent deformation model for the subgrade of the pavement, considering the influence of the dissipated energy in the material.

A 3D finite element model was developed using SV-Solid(SoilVision, 2009). A typical pavement structure was evaluated under the following conditions: Not significant influence of the water table, surface temperature of 20°C, and a vehicle speed of 40 km/h. Figure 2 shows the pavement structures and the truck with a special axle configuration considered in the study. Pavement section presented in Figure 2 was also used during the full-scale testing. Pavement materials used to correspond to those established in the current standards in the Province of Quebec (BNQ, 2002).

3.1. Material properties

The dynamic modulus master curve was adjusted to the sigmoidal function described in the following equation(ARA Inc, 2004):

[2]

$$\log|E^*| = \delta + \frac{\alpha}{1 + e^{\beta+\gamma(\log f_r)}}$$

Where E^* is the dynamic modulus, f_r is the reduced frequency at the reference temperature, δ and α are fitting parameters for a given set of data, and β and γ are parameters describing the shape of the sigmoidal function. The equation [3] provides the general form of the shift factors.

[3]

$$\log f_r = \log f + a_1(T_R - T) + a_2(T_R - T)^2$$

Where, f is the loading frequency at the test temperature in Hz, T_R is the reference temperature in °C, and T is the temperature of interest in °C. Variables associated with equations [2] and [3] for the materials used in this study are shown in table 1.

Similarly, the Uzan model was used to adjust the resilient modulus of the granular materials and soil. The general constitutive model is presented in equation [4] (ARA Inc, 2004; Doré and Zubeck, 2009):

[4]

$$M_r = k_1 p_a \left(\frac{I_1}{p_a}\right)^{k_2} \left(\frac{\tau_{oct}}{p_a} + 1\right)^{k_3}$$

With,

[5]

$$I_1 = \sigma_1 + \sigma_2 + \sigma_3$$

[6]

$$\tau_{oct} = \frac{1}{3}\sqrt{(\sigma_1 - \sigma_2)^2 + (\sigma_1 - \sigma_3)^2 + (\sigma_2 - \sigma_3)^2}$$

Where, M_r is the resilient modulus, I_1 the bulk stress, τ_{oct} the octahedral shear stress, p_a the reference pressure (100 kPa), k_1 , k_2 and k_3 are experimentally determined constants. The variables defined for the materials used are shown in table 2.

4. Pavement mechanical response with SHL conditions.

Pavement mechanical response is a fundamental part of the analysis. Conditions described by a typical SHL vehicle (see Figure 2) were simulated. Three references to the stress conditions were defined: two axes (1 and 2) parallel to the direction of circulation of the vehicle, and one axis perpendicular to this direction (3). Results at the top of the subgrade under this reference axes are compared in order to define the critical conditions for permanent deformation caused by the loading setting. The meshing, loads position and reference axes are shown in Figure 3. A summary of the resulting conditions at the top of the subgrade is shown in Figure 4, described by the deviatoric stress ($q = \sigma_1 - \sigma_3$), with σ_1 and σ_3 as the maximum and minimum principal stresses respectively, and the corresponding strains.

In the results, it can be appreciated that the transit of an SHL truck generates a continuous solicitation (without rest) in the structure, both in stress and strains. Similarly, and as expected, the axle's configuration with a set of 8 wheels and 273 kN per axle generate higher solicitations than the configuration of 4 wheels and 370 kN per axle. In addition, strain levels are higher in the outermost wheel line than in the internal ones.

It can be seen that the transverse stress distribution in a multi-wheel configuration cause that the confinement stress (σ_3) is higher in the areas in the area under the action of this wheel configuration (see Figure 4b). The increase of the confinement stress in this area of influence means a lower susceptibility to permanent deformation of the material, since the resistance to deformation is considered directly proportional to the level of confinement (Tseng and Lytton,

1989). Given this, it can be indicated that the area most susceptible to permanent deformation, and where the analysis should focus, is on the edges of the multi-wheel set.

Using the results of the finite element model, the relationship between stress and strains were also studied as a basis for quantifying the energy dissipated in non-conventional axle configurations. Figure 5 shows the stress-strain ratio under the SHL truck used in the simulation (see Figure 2). In this case, the quantification of the dissipated energy cannot be defined in a trivial way; however, the method to calculate the dissipated energy in this type of vehicle exceeds the objectives of this article; nonetheless, with the data obtained can be appreciated that load conditions that generate a dissipated energy with magnitude similar to these can be defined. In addition, a difference between dissipated energy caused by the external and internal wheels in the axle configuration is expected (see Figure 5), indicating that the influence of the load will not be homogeneous and that is defined by the axial configuration of the vehicle itself.

5. Development of Permanent Deformation Model

Several models have been developed to predict permanent deformation behaviour by considering the number of load cycles(Lekarp & Dawson, 1998), stress level (Rahman and Erlingsson, 2015) and a combination of both criteria(Lekarp et al., 2000; Lekarp and Dawson, 1998). In addition, based on shakedown theory, several researchers have developed methods for calculating either shakedown load or permanent deformation (Boulbibane et al., 2005). Leiva et al.(Leiva et al., 2017) developed an auto-regressive model the total permanent deformation in the pavement structure, using data from a heavy vehicle simulator (HVS), considering indirectly the stress history in the structure using the number of load applications and the elastic response given by a deflection test (FWD).

The models available in the literature are normally developed using cyclic triaxial tests, and in some cases experimentally in test sections. The common objective is to predict the accumulation of permanent deformation in the structure; however, since the passage of a vehicle with special axles is not a fixed event in the road network, for this study, it is considered that the rate of deformation given by a particular stress condition is a more rational variable to model. Based on this, an analytical equation can be defined for the calculation of the permanent deformation accumulation using the deformation rate:

[7]

$$\varepsilon_p^i = \bar{\varepsilon_p}^i \cdot N^i \cdot h + \varepsilon_p^{i-1}$$

Where, ε_p^i and ε_p^{i-1} are the cumulative deformation cause by the dissipated energy in cycle i and $i-1$ respectively; h is the thickness of the layer to be considered; N^i is the number of load

repetitions in cycle i; and $\bar{\varepsilon_p}^i$ is the rate of deformation defined by the stress conditions in cycle i. Equation [7] should be used as an iterative function, where each variable can be recalculated for the next cycle, and each cycle is representing a number of load repetitions with similar stress state.

Based on experimental information, the following analytical-empirical model is proposed for the prediction of the permanent deformation rate using dissipated energy as input:

[8]

$$\bar{\varepsilon_p} = \frac{d\varepsilon_p}{1 + e^{\frac{\sum W_N - W_0}{dx}}} + \varepsilon_p^{ps}$$

Where, $\bar{\varepsilon_p}$ is the rate of deformation given a certain accumulation of dissipated energy and stress stage; $\sum W_N$ is the accumulation of dissipated energy in the structure; is the $d\varepsilon_p$ is the amplitude of the range of the permanent deformation rate; $\varepsilon_p^{ps}$is the deformation rate associated with a state of equilibrium shakedown of the material, W_0 and dx are shape parameters for the model. In Figure 6a, it can be seen the model fit in a single stress state condition obtained in a laboratory test.

5.1. Full-scale Testing

The model described in equation [8] was used to adjust the measured deformation rate under full-scale test conditions. The test was performed by increasing the magnitude of applied load every certain number of load cycles, from 40 kN to 80 kN. Figure 6b shows the resulting adjustment on the subgrade of the EB150 pavement structure (see figure 2b). Different stress levels were recorded, given this, equations to determine the variables in the equation [8] in a multistage stress condition were defined according to the conditions described by the deviatoric stress ($q = \sigma_1 - \sigma_3$) and the mean stress ($p = [\sigma_1 - 2\sigma_3]/3$). Models for each variable are presented in Table 3.

5.2. Laboratory Testing

Cyclic triaxial tests were performed on the subgrade material following the EN-13286-7 test procedure(CEN, 2003). Conditions established for a low-stress level evaluation were defined for the test. Equation [8] parameters were defined using the laboratory measurements, and equations shown in Table 3 were used to consider the multistage stress condition. Comparison of results for parameters defined in each condition (i.e. full-scale and laboratory) are shown in Figure 7.

Figure 7 shows that there is a linear correlation between laboratory and full-scale measurements. This trend is different in each confinement level case, so a laboratory test at a defined confinement level would be sufficient to obtain parameters analogous to those expected in the field. In this study, confinement stress of 100 kPa offers the best results for the definition of ε_p^{ps}, W_0, and dx; while with a confinement stress of 20 kPa better results for $d\varepsilon_p$ are obtained.

6. Conclusions

SHL vehicles, normally associated with special axial configurations, cause particular mechanical response on the pavement structure. The most critical condition for permanent deformation, defined by this special axle configuration, are those defined by the wheels on the external borders of the axle configuration. This is due to the fact that in the active zones of the inner wheels the confinement level increases, associating this condition with greater resistance to the development of permanent deformation.

The dissipated energy is a rational variable to maintain in a same context of analysis the laboratory measurements, numerical simulations and field expected values, and can result in a useful reference variable for the definition of simplified load conditions that better model the effect of special axial configurations. However, quantification of the energy dissipated in vehicles with non-conventional axles is a topic that needs more study to close the gap between theory and practice.

A model for calculating the change in the rate of permanent deformation given the accumulation of energy dissipated in the material was presented. This model was developed by coupling measurements of cyclic triaxial tests and full-scale measurements with an HVS. This model demonstrates that there is a clear correlation between the dissipated energy and the change in the rate of permanent deformation caused by the stress levels, and thus with the development of permanent deformation in the material.

Given the difference between the energy dissipated between the external and internal wheels of the multi-wheel axle configuration (see Figure 5), the trend described by the analytic model developed (see equation 8) and the confinement levels develop under special axle configuration (see Figure 4d), it can be inferred that the development of permanent deformation under the special conditions presented in this paper will not be homogeneous and that the most critical condition for the deformation is given by the outermost wheel in the multi-wheel axle.

Future research should confirm these findings by applying the principles described in this paper to other case studies, in order to validate the trends and models presented. Similarly, more

research is needed to close the gap between the calculation of dissipated energy and its practical applications to pavement engineering.

7. References

ARA Inc, 2004. Guide for the Mechanistic-Empirical Design of New and Rehabilitated Pavement Structures (Final report No. NCHRP 1-37A). Transportation Research Board of the National Academies, Washington, D.C.

BNQ, 2002. NQ 2560-114: Travaux de génie civil - Granulats. Bureau de normalisation du Québec, Québec.

Boulbibane, M., Collins, I., Ponter, A., Weichert, D., 2005. Shakedown of unbound pavements. Road Materials and Pavement Design 81–96.

CEN, 2003. Unbound and hydraulically bound mixtures - test methods: Cyclic load triaxial tests for unbound mixtures. Comité Européen de Normalisation.

Chen, D.-H., Fernando, E., Murphy, M., 1996. Application of Falling Weight Deflectometer Data for Analysis of Superheavy Loads. TRANSPORTATION RESEARCH RECORD 8.

Chen, X., Lambert, J.R., Tsai, C., Zhang, Z., 2013. Evaluation of superheavy load movement on flexible pavements. International Journal of Pavement Engineering 14, 440–448. https://doi.org/10.1080/10298436.2012.690519

Doré, G., Zubeck, H.K., 2009. Cold regions pavement engineering. ASCE Press ; McGraw-Hill, Reston, VA : New York.

Hajj, E., Siddharthan, R., Nabizadeh, H., Elfass, S., Nimeri, M., Kazemi, S., Batioja-Alvarez, D., Piratheepan, M., 2018. Analysis Procedures for Evaluating Superheavy Load Movement on Flexible Pavements, Volume I: Final Report (Final Report No. FHWA-HRT-18-049). U.S. Department of Transportation (USDOT).

Jooste, F., Fernando, E., 1995. Development of a procedure for the structural evaluation of superheavy loads routes (No. 1335– 3F). Texas.

Leiva, F., Pérez, E., Aguiar, J., Loría, L., 2017. Permanent deformation model for pavement condition assessment Modelo de deformación permanente para la evaluación de la condición del pavimento 32, 10.

Lekarp, F., Dawson, A., 1998. Modelling permanent deformation behaviour of unbound granular materials. Construction and Building Materials 12, 9–18. https://doi.org/10.1016/S0950-0618(97)00078-0

Lekarp, F., Isacsson, U., Dawson, A., 2000. State of the Art. II: Permanent Strain Response of Unbound Aggregates. Journal of Transportation Engineering 126, 76–83. https://doi.org/10.1061/(ASCE)0733-947X(2000)126:1(76)

Maggiore, C., Airey, G., Marsac, P., 2014. A dissipated energy comparison to evaluate fatigue resistance using 2-point bending. Journal of Traffic and Transportation Engineering (English Edition) 1, 49–54. https://doi.org/10.1016/S2095-7564 (15)30088-X

Rahman, M.S., Erlingsson, S., 2015. A model for predicting permanent deformation of unbound granular materials. Road Materials and Pavement Design 16, 653–673. https://doi.org/10.1080/14680629.2015.1026382

Shen, S., Airey, G.D., Carpenter, S.H., Huang, H., 2006. A Dissipated Energy Approach to Fatigue Evaluation. Road Materials and Pavement Design 7, 47–69. https://doi.org/10.1080/14680629.2006.9690026

SoilVision, 2009. SVOFFICE 2009 Help Manual.

Tseng, K., Lytton, R., 1989. Prediction of permanent deformation in flexible pavements materials 154–172.

Van Dijk, W., Visser, W., 1977. Energy approach to fatigue for pavement design. Association of Asphalt Paving Technologists Proc. 1–40.

Tables

Table 1. Variables of the model of dynamic modulus master curve for the asphalt mixture.

Material	Type	δ	α	β	γ	a_1	a_2
Asphalt concrete	EB-10C	0.668	3.716	-1.133	-0.608	-0.135	7.82E-4

Table 2. Variables of the Uzan model for the granular material and soil.

Material	Type	k_1	k_2	k_3
Base	MG20	1683	0.732	-0.144
Subbase	MG112	1297	0.702	-0.049
Subgrade	SM	447	0.740	-0.160

Table 3. Model variables associated with states of stress in the structure: Subgrade material.

Model	α_1	α_2	α_3	R^2
$\varepsilon_p^{ps} = e^{\alpha_1+\alpha_2\left(\frac{q}{p}\right)+\alpha_3\left(\frac{q}{p}\right)^2}$	-9.03	1.10	1.14	0.980
$d\varepsilon_p = \alpha_1 \times e^{\alpha_2(q)}$	0.001	0.107	-	0.987
$W_0 = \alpha_1 \times {\alpha_2}^{(q)}$	1043.9	298.79	-	0.776
$dx = \alpha_1 \times {\alpha_2}^{(q)}$	1533.5	50.55	-	0.977

Figures

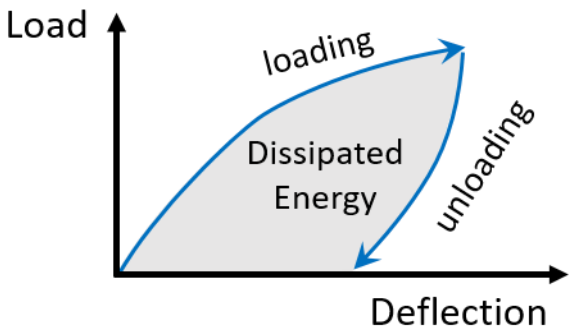

Figure 1. Illustrative representation of the dissipated energy in materials.

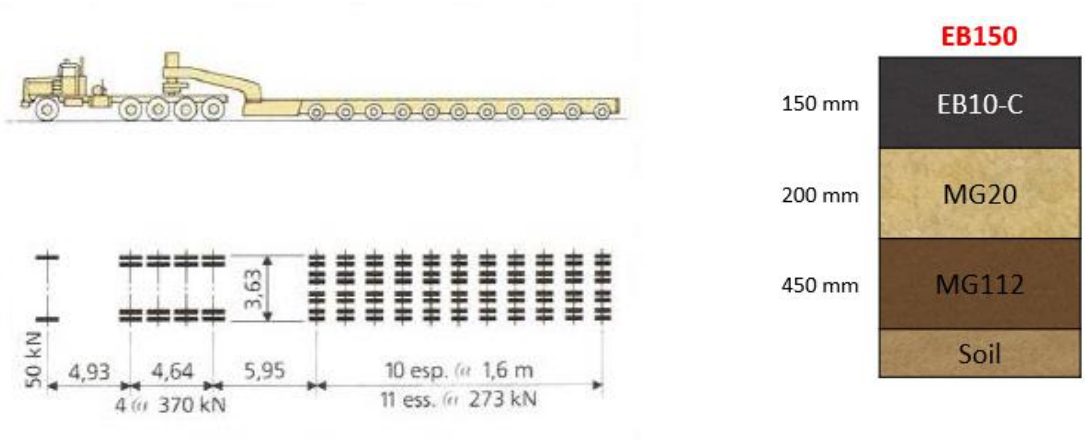

(a) *(b)*

Figure 2. (a) Multi-axle truck of reference (b) Pavement structure considered during the study.

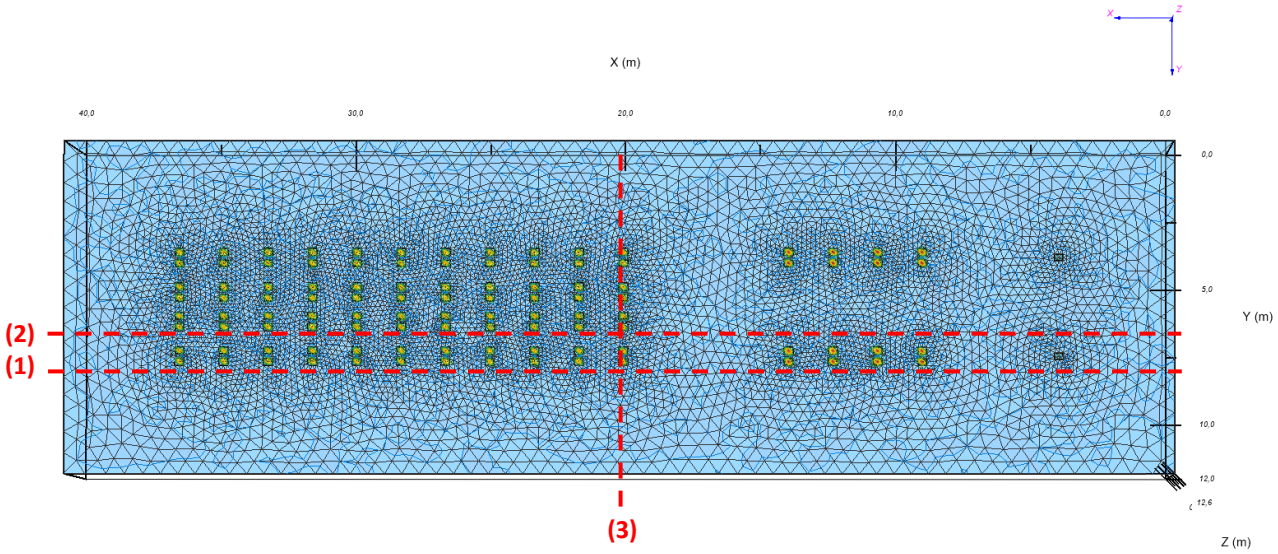

Figure 3. Meshing in the finite element models and position of reference lines for the analysis.

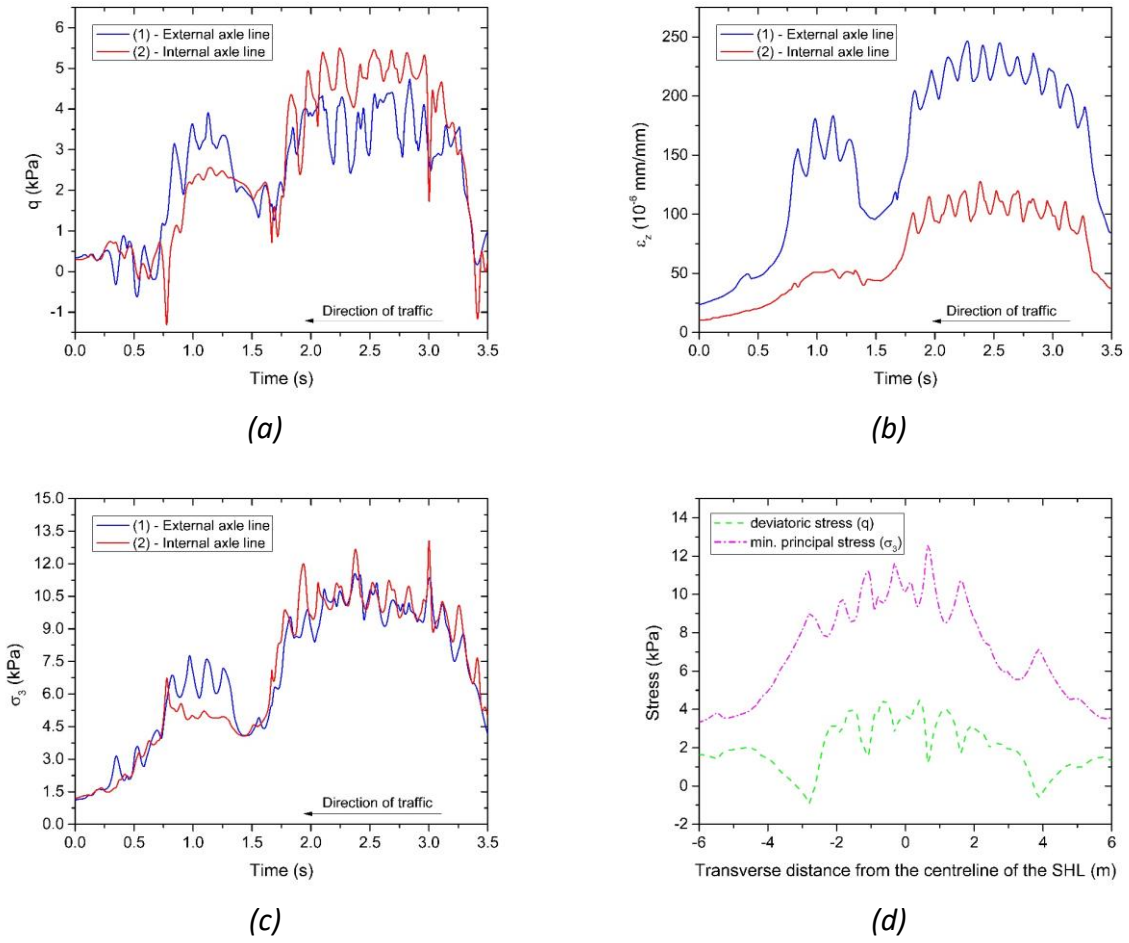

Figure 4. Mechanical response at the top of the subgrade, resulting from SHL simulation.

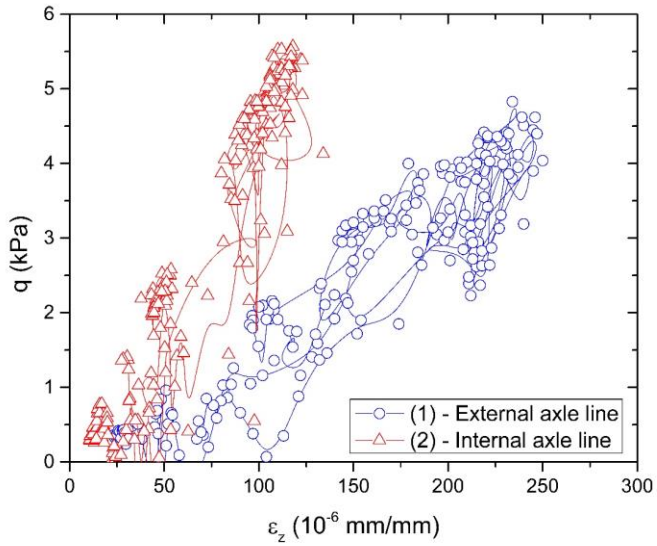

Figure 5. Stress-strain, at the top of the subgrade, under the passage of an SHL truck.

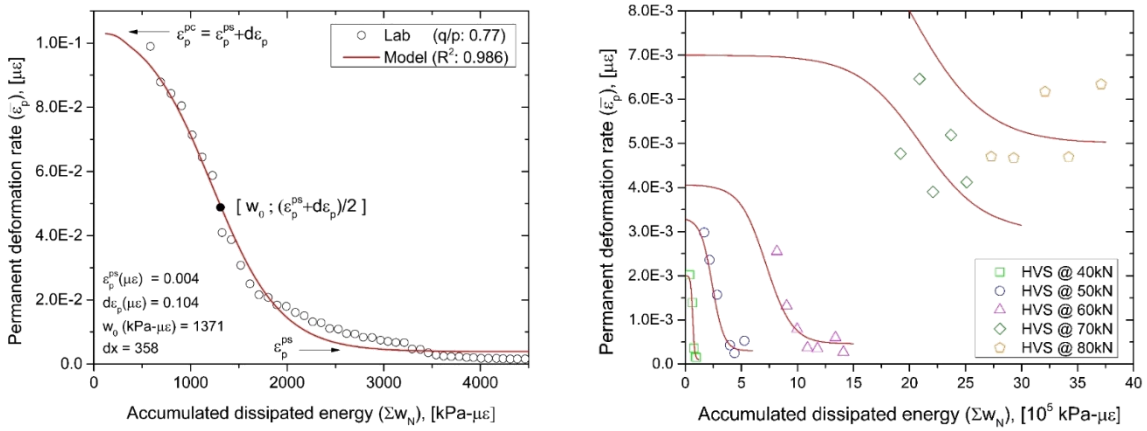

(a) *(b)*

Figure 6. Model adjusted: (a) Single stress stage in the laboratory (b) Multi-stage stress condition in the HVS.

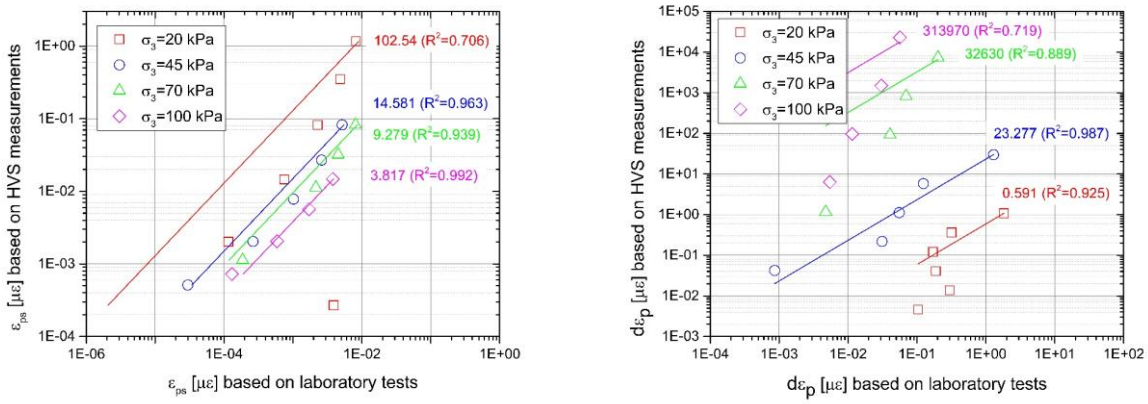

(a) *(b)*

(c) *(d)*

Figure 7. Correlation between model parameters adjusted to laboratory conditions and real scale conditions (HVS).